Student thesis series INES nr 406

Spatiotemporal reconstructions of black carbon, organic matter and heavy metals in coastal records of south-west Sweden

Marcus Rudolf

2016
Department of
Physical Geography and Ecosystem Science
Lund University
Sölvegatan 12
S-223 62 Lund
Sweden

Marcus Rudolf (2016).
Spatiotemporal reconstructions of black carbon, organic matter and heavy metals in coastal records of south-west Sweden
Spatiotemporala rekonstruktioner av deposition av sot, organiskt material och tungmetaller i sediment längs Sydvästsveriges kust
Master degree thesis, 30 credits in *Subject of degree*
Department of Physical Geography and Ecosystem Science, Lund University

Level: Master of Science (MSc)

Course duration: *January* 2016 until *June* 2016

Disclaimer

Spatiotemporal reconstructions of black carbon, organic matter and heavy metals in coastal records of south-west Sweden

---

Marcus Rudolf

Master thesis, 30 credits, in
Physical Geography and Ecosystem Analysis

Karl Ljung
Department of Geology

Exam committee:
Johanna Stadmark, Department of Geology
Nadine B. Quintana Krupinski, Department of Geology

Abstract

This study presents reconstructions of black carbon (BC), including spheroidal and amorphous carbonaceous particles (SCP and ACP), organic matter (OM; total organic carbon, TOC; total nitrogen, TN; total sulfur, TS), and heavy metals (Fe, Zn, Pb, Cu, As and Hg) in coastal sediments off the south-west coast of Sweden. Sediment records from eight stations along a north-south transect off the south-west of Sweden were retrieved. Samples of 0-1 cm depth from each station representing recent depositions and a sediment core from the Öresund extending back to approximately AD 1912 were analyzed.

For investigations of BC, the samples were pre-treated using the chemothermal oxidation (CTO) method. For the particle counting of SCP and ACP, the samples were pre-treated chemically before they were analyzed under a microscope. The burial fluxes of BC, SCP and ACP showed an increasing trend since the start of the record in 1912 with a slight decrease of the trend between 1965 and 1986. This decrease seemed to be the result of some legislative actions to improve the air quality since the beginning of the 1960s. The BC burial flux was already high from the early 1990s with the highest peak about 636 µg/cm^2/yr in year 2008. Looking at the trend from 1912 to 2011 the trend of BC and SCP and ACP burial fluxes are positive with a slight decrease from the 1960s until late 1980s.

OM and calcium carbonate ($CaCO_3$) were studied as biogeochemical markers for oxygen bottom water conditions and biological activity, respectively. OM dropped in the 1960s until 1986 and $CaCO_3$ started to increase from 1965 until the top of the record. $CaCO_3$ and OM could be evidence of BC oxidation in the Öresund record and might have caused underestimation of the BC burial flux between the 1960s and 1990s because of more oxic bottom water conditions. Samples analyzed for heavy metal concentrations were ground in a mortar and analyzed with an XRF scanner. All trends of heavy metals except Fe showed strong increase from 1960 and lasted partly until the early 1990s. Fe displayed a very similar pattern as TS. There were no or low correlations between any burial flux of BC, SCP and ACP and any heavy metal pointing out that heavy metals were mainly produced and emitted from a different source or process than combustion.

Contents

List of Figures

List of Tables

1 Introduction

Human pollution (e.g. energy production, traffic exhaust, heavy industry) emits black carbon (BC) and heavy metals. Although BC is also produced naturally by wildfires, this human pollution can affect the environment and may have negative effects as, for example, threatening the development, reproduction and life of organisms (Lippmann & Albert, 1969; Oberdörster & Yu, 1990; Valette-Silver, 1993). The deposition of heavy metals in the environment has been part of the human pollution history ever since the beginning of the processing of ores (Renberg et al., 1993). Emission and deposition of BC and heavy metals have increased drastically since the industrial revolution in the mid-19th century, as a consequence of coal and oil burning; especially, in dense human-settled areas and highly industrialized regions (Förstner & Wittmann, 1981). This deposition of pollution took place in the Swedish shelf, including the Öresund, and has been archived in sediment records. This study assessed the depositions of BC, and heavy metals (e.g. Fe, Zn, Pb, Cu, As and Hg) for similar patterns in the sediments (Adriano, 2001; Bryan & Langston, 1992; Carbone et al., 2015; Sokhi et al., 1990). To date, projects in Sweden were conducted on surface samples for estimations of the BC content in the recent coastal shelf (Gustafsson & Gschwend, 1998; Sánchez-García et al., 2012) and for reconstruction of the historical trends in lacustrine (Elmquist et al., 2007) sediments. In an unique approach, this project aimed to compare reconstructions of the spatial and historical depositions of

1. BC (including carbonaceous particles) and heavy metals, and
2. organic matter (OM) and calcium carbonate ($CaCO_3$)

from coastal sediments off the Swedish south-west coast, including a dated sediment record from the Öresund to comprehend the trends of the pollution development in the south-west of Sweden.

2 Background

2.1 Pollution history of the Öresund

Anderberg (2009) stated that since the beginning of the 20th century, industrial growth dominated in Copenhagen and Malmö, Denmark's capital and Sweden's third biggest city, respectively. Around the 1949, Copenhagen was the most dominant industrial area in Denmark and while Skåne was still the most diverse industry in Sweden, which was going hand in hand with urbanization. From 1900-1950, urban population of the Öresund region increased from 800,000 to 2 million, which took mostly place in Greater Copenhagen and in

the Swedish cities along the sound, i.e. Malmö, Helsingborg and Landskrona. This trend continued to more than 3.6 million in 2005. However, national importance of Skåne dropped as other Swedish regions gained significance as export-industries (e.g. metal) in the second half of the 20th century. Malmö and Trelleborg kept their position as industrial centers and Höganäs similarly evolved to an important center for metals (Anderberg, 2009). These developments caused increasing pollution loads in this region, with a lot of sewage and waste deposited in the Öresund strait.

2.2 Black carbon

BC is an aerosol and is produced by incomplete combustion of fossil fuels (e.g. power plants, traffic exhausts from vessels and cars, and industry) and wildfires (Forbes et al., 2006; Libes, 2009; Rose & Juggins, 1994). It is introduced to the environment via aeolian and fluvial transport, before it deposits in marine sediments (Forbes et al., 2006). Production of BC is equivalent to around 1-3 % of the production of total carbon dioxide (CO_2), which is produced globally during combustion (Druffel, 2004) and plays a crucial role as cloud condensation nuclei in cloud formation, affects Earth's albedo and, thus, Earth's radiative balance. Due to these physical characteristics, it scatters and absorbs solar radiation (Bond et al., 2013). If BC is deposited on ice- and snowfields in high latitudes, it can significantly lower the albedo (Chung et al., 2005; Ramanathan & Carmichael, 2008). The black carbon continuum model (BCCM; see figure 1) has a diverse mixture of residues with contrasting chemistry and each spectrum has its own recalcitrance to further physical and chemical degradation (e.g. oxidation), in which soot, spheroidal carbonaceous particles (SCP), and charcoal are the most resistant fractions, respectively (Forbes et al., 2006; Hedges et al., 2000; Masiello, 2004; Ruppel et al., 2015).

Once BC is washed out from the atmosphere to the Earth's surface and buried in soils and sediments, it may affect as well the turnover of the organic carbon (OC) pool if BC (as part of OC) leaves the biological and enters instead the geological cycle (Chung & Seinfeld, 2002; IPCC, 2013; Ramanathan & Carmichael, 2008). Forbes et al. (2006) concluded that inert charcoal (named as amorphous carbonaceous particles (ACP) in this project), produced by wildfires, represents less than 3% sink in the global carbon budget with a slow turnover and more than 80 % of charcoal remains in the proximity to the production area. The river-estuary systems play an important role in the transport of BC to the oceans from the areas where it is produced (Mannino & Harvey, 2004). Suman et al. (1997) modeled that more than 90 % of charcoal deposition in the oceans takes place on the continental shelves and only a minor portion drifts to the deep ocean (Forbes et al., 2006). Thus, higher concentrations of BC in sediments can be expected in coastal areas close to sources of pollution, such as the Öresund region.

SCP and soot and are mainly produced by incomplete combustion of fossil fuels at high temperatures above 1000 °C in power plants for energy production and traffic exhaust. The small soot and SCP are capable of travelling in the atmosphere for several 1000 km (Ruppel, 2015). While soot is produced in high temperatures of all kinds of fuels, SCP are only produced in combustion of fossil fuels (i.e. oil and coal) (Ruppel, 2015). Thus, they are a suitable geochronology tool and a proxy for atmospheric pollution and the industrial development during the Anthropocene (Forbes et al., 2006; Rose, 2015).

2.2.1 Terminology

The term black carbon (BC) is used in this study as the fraction of the black carbon continuum model that is surviving the chemical and thermal oxidation at 375 °C, and measured using an elemental analyzer. It probably includes soot and spheroidal carbonaceous particles (SCP), which are unlikely to degrade during the oxidation pretreatment. However, SCP-mass was not quantified in this study, but can be assumed to be a minor part of the BCCM (Ruppel, 2015). Amorphous carbonaceous particles (ACP) were identified under a light microscope, and are most likely charcoal (compare Thevenon & Anselmetti, 2007).

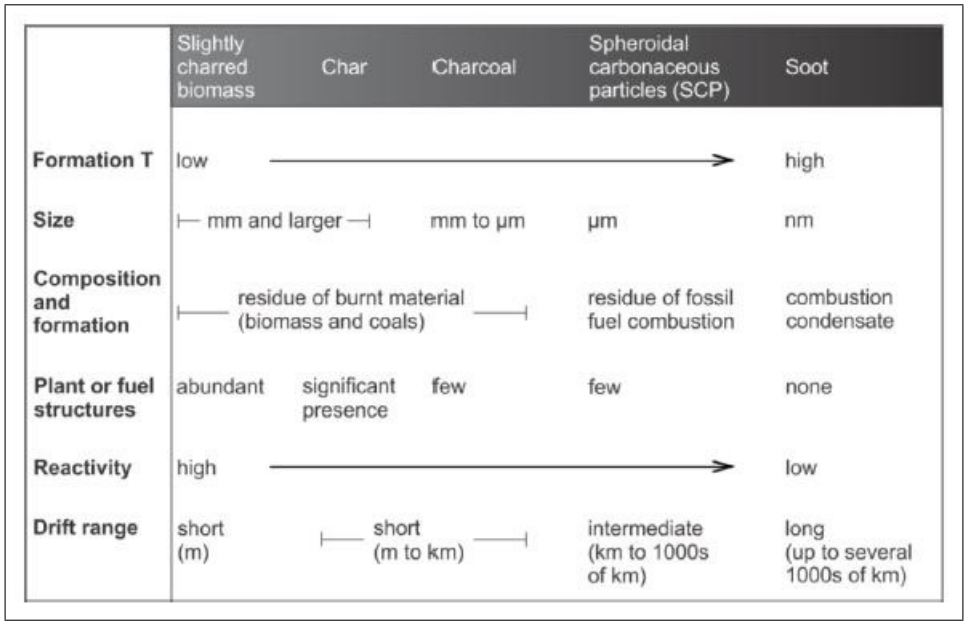

Figure 1: Black carbon continuum model (Rose & Ruppel 2015, modiefied fromHedges et al. 2000; Masiello 2004; reproduced with permission of Springer Science+Business Media)

2.3 Other products of combustion

Fossil fuel combustion is also the most significant source of S, which is mostly emitted in form of sulfur dioxide (SO_2), but also the aerosol sulfate ($SO_4{}^{2-}$) (IPCC, 2013; Smith et al., 2001). SO_2 reacts with oxygen and water in the atmosphere to sulfuric acid (H_2SO_4) and sulfurous acid (H_2SO_3), which have a low pH and are components of acid rain. This can affect the environment due to acidification, causing rock weathering, and significant damages to buildings (Li et al., 2008; Sanderson et al., 2006; Srivastava et al., 2001). Metal mining and smelting since the 20th century and fossil fuel burning are furthermore sources of dramatically increased emissions of heavy metals (Adriano, 2001; Callender, 2014; Valette-Silver, 1993). As the pathways of BC, the pathways of heavy metals are aeolian and fluvial into the environment (Callender, 2014). The concentration of heavy metals can be controlled due to equilibria reactions of deposited heavy metals in the sediments and dissolved heavy metals in the overlying waters. The concentrations of most heavy metals in sediments are much higher than in the water. Furthermore, even more toxic organic (methyl) compounds can be formed by some heavy metals (e.g. As, Hg and Pb) during their adsorption to sediment particles (Bryan & Langston, 1992). The bioavailability of heavy metals can have significant effects on organisms and can already be toxic, carcinogenic and even lethal for organisms in moderate concentrations and, additionally, bioaccumulate in the food web (Adriano, 2001; Callender, 2014; Dave & Dennegård, 1994; Rae, 1997; Rosenberg et al., 1996; Valette-Silver, 1993). Although, heavy metals are not only in the environment due to pollution, they also appear naturally in uncontaminated sites in mineral lattices and have to be considered as natural background (Rae, 1997).

2.4 Hydrography and deposition

The Öresund covers a total area of ca. 2,300 km^2 (Lumborg, 2005) and has a complex hydrography; sometimes with opposite directed currents in two- or three-layer stratifications (Sayin & Krauss, 1996). The Öresund contains brackish water with a salinity of around 10 due to the freshwater flux from rivers into the the Baltic Sea and the more saline water from the North Sea with a salinity around 30, which furthermore results in the establishment of a strong halocline. Additionally, the Drogden Sill hinders the saline water from the north to pour in to the Baltic Sea (Lintrup & Jakobsen, 1999).

The transport and deposition of fine-grained sediments are important factors of pollution in marine environments Lumborg (2005). Pollutants as heavy metals and BC tend to bind to these fine-grained sediments. The size and the surface of the particles play key roles in the adsorption of pollutants (Rae, 1997). The

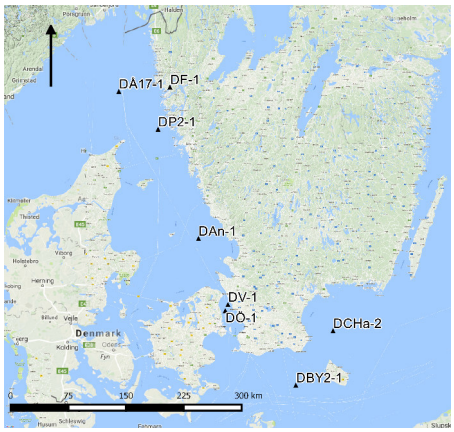

Station ID	Latitude	Longitude	Marine province
DÅ17-1	58° 16.30	10° 30.49	Skagerrak
DF-1	58° 19.10	11° 32.40	Skagerrak
DP2-1	57° 51.95	11° 18.00	Skagerrak
DAn-1	56° 40.13	12° 70.00	Kattegat
DV-1	55° 55.59	12° 42.66	Öresund
DÖ-1	55° 51.47	12° 41.05	Öresund
DBY2-1	55° 00.00	14° 04.95	Arkona Basin
DCHa-2	55° 37.60	14° 50.00	Bornholm Sea

Figure 2: Positions and coordinates of sampling stations off the south-west coast of Sweden (see Charrieau et al., tted). DF-1 is located in the Gullmarn Fjord, whose outflow enters the Skagerrak. DV-1 is north and DÖ-1 is south off the island Ven in the Öresund. Coordinates for DÖ-1 were estimated.

deeper parts of the northern Öresund (including station DV-1) consists of fine cohesive sediments, while the shallower parts incorporate more boulders and sandy areas (Lumborg, 2005).

3 Methods

3.1 Sediment sampling and material

Eight stations in the Skagerrak (including one from the Gullmarn Fjord), Kattegat, Öresund, Arkona Basin and Bornholm Sea were sampled by Charrieau et al. (tted). Samples were recovered with a Gemini gravity corer (inner diameter of 9 cm). The cores were sub-sampled in 1 cm-intervals on the ship and freeze-dried. The sub-samples of 0-1 cm depth of each core and two simultaneously retrieved and parallel records of 24 (G-core) and 28,5 cm depth (H-core) from the Öresund were used for analyses.

3.2 Age model and sedimentation rate

Charrieau et al. (tted) dated the core DV-1 G using ^{210}Pb by (Appleby, 2001; Appleby & Oldfieldz, 1983). The sub-samples were measured with an ORTEC HPGe (High-Purity Germanium) Gamma Detector at the Department of Geology at Lund University, Sweden which reported the age model. ^{210}Pb has a half-life of 22.26 years and it can be dated for ages from 1-150 years. The unsupported ^{210}Pb is washed out from the atmosphere and is the product of ^{222}Rn, which evaporates from the land surface. The artificial tracer ^{137}Cs was measured for an independent validation of ^{210}Pb. ^{137}Cs has a half life of 30.17 years and is produced by the process of nuclear fission of ^{235}uranium and reaches peaks in 1963 due to nuclear bomb tests and 1986 due to the Chernobyl catastrophe.

Self-absorption corrections were created for ^{210}Pb on each sample using the technique from Cutshall et al. (1983). For the ^{210}Pb dating, the activity of ^{210}Pb was measured at its gamma peak at 46,5 keV, the ^{224}Ra was determined via its granddaughters ^{114}Pb at 295 keV and 352 keV and ^{114}Bi at 609 keV. The ^{137}Cs activity was measured at the 662 keV gamma peak. The age model and the calculated sedimentation rate of the G-core were used for the H-core assuming the dates of the samples were the same. The lowermost 4 cm of the H-core had to be extrapolated from the sedimentation rate and age model because the G-core was shorter.

3.3 Black carbon and organic matter

Since BC is resistant to oxidation (Elmquist et al., 2006; Hammes et al., 2007), it is possible to measure the BC fraction by using chemical and thermal oxidation to remove organic and inorganic carbon. The procedure followed the chemothermal oxidation-method (CTO) as described in Elmquist et al. (2004) and Gustafsson

et al. (2001). The freeze-dried samples of the H-core were finely ground with a mortar and pestle. About 10 mg of sediment was prepared for in situ thermal and acid treatment in pre-combusted silver (Ag) capsules. The samples were combusted in a muffle oven for 18 h with a stable increasing ramp of 4 h until 375 °C were reached. Inorganic carbon was removed by treatment with 1 M HCl, added in steps (2 x 20; 30; 50; 100 µL), and heated to 50 °C. This step was carefully done to prevent any drying out or spilling over of the samples due to strong reactions in the capsules. The samples were heated until complete evaporation of the acid, before the silver capsules were closed. The remaining carbon content was measured on an elemental analyzer.

For the measurement of total organic carbon (TOC), 10 mg of each sample have been analyzed and pre-treated with hydrochloric acid (HCl) in the same amounts as for the BC samples and measured in an elemental analyzer. Total sulfur (TS) content was analyzed in a separate run where ca. 5 mg of each sample was filled in tin capsules and vanadium pentoxide was added as catalyst. For more simple purposes TS refers to OM in this thesis, although TS contains as well inorganic sulfur. During the TS run, total carbon (TC) and nitrogen (TN) contents were analyzed as well. The content of calcium carbonate ($CaCO_3$) was estimated as the difference of TC and TOC.

3.4 Spheroidal and amorphous carbonaceous particles

Spheroidal and amorphous carbonaceous particles (SCP and ACP, respectively) are microscopic particles and can be counted using a light microscope (figure 3). In this project, charcoal particles (compare Thevenon & Anselmetti, 2007) were investigated but due to an uncertainty about their identification, these particles were named amorphous carbonaceous particles (ACP). Carbonaceous particles are resistant to oxidation, and samples were treated with nitric (68 % NHO_3), hydrofluoric (HF), and hydrochloric acid (1M HCl) to remove organic matter, siliceous material, and carbonates, respectively, following the protocol of Rose (1990,9).

About 0.1 - 0.15 g of freeze dried material was weighed in polypropylene test-tubes. Carbonates were removed using 1 M HCl, which was added carefully in small steps to avoid too vigorous reaction and loss of material, and heated for 2 h. Organic matter was removed with nitric acid, added in two steps of 2.5 ml, and left over night. On the next day 1.5 ml of nitric acid were added again and heated to 90 °C for two hours. Minerogenic matter was removed using 8 ml 40 % HF per sample and heated to 90 °C for 3 hours before finally, 3 ml of 6 M HCl were added to the samples and heated to 90 °C for 2 hours. After the acid treatments, the samples were rinsed with de-ionized water and centrifuged. Before the residue was weighed and transferred to labeled vials for storage, it was rinsed with de-ionized water for three times.

One drop of each residue was prepared on a slide for counting. The weight of the drop was used to quantify the particles/gram dry weight (gdw). For both, SCP and ACP, all particles were counted on the whole cover slip. Particles larger than 10 µm were counted at a 200-fold magnification. After Rose's suggestion (1994), only particles of at least half a spheroidal particle were counted. Following this manual, such a half particles were identified when the microscopic focus centered on the spheroidal and often oily character a SCP.

3.5 Burial fluxes

Burial fluxes of BC, SCP and ACP were calculated. To estimate the burial fluxes, the results were used in the formula:

$$F_{BC;SCP;ACP} = C_{BC;SCP;ACP} \cdot \omega \cdot \rho \tag{1}$$

where F is the burial flux of soot-BC (µg/cm^2/yr), SCP or ACP (particles/cm^2/yr), C is the measured BC (wt%), SCP or ACP concentration (particles/gdw) and ω is the sedimentation rate (cm/yr) (1). ρ is the density of the dry sediment (g/cm^3), which was measured in the G-core down to a depth of 24 cm. The burial fluxes of the lowermost four samples of the H-core have been calculated using the mean of the G-core densities.

3.6 Heavy metals

The trends of heavy metals can be used for reconstructions of past pollution (Rae, 1997; Valette-Silver, 1993) and are of interest since they indicate variations in the redox system of the sediments and bottom waters. Samples were analyzed for heavy metals using a handheld XRF scanner (Danielsson et al., 1999; Mejía-Piña et al., 2016). The samples were ground in a mortar into a homogeneous powder before they were prepared in sample cups, pressed manually, and sealed with an elastic foil. The samples were measured in three intervals with different X-ray radiations for measuring various heavy metals. The heavy metals Fe, Zn, Cu, Pb, As and Hg were chosen to show the deposition of these pollutants in the samples because they are also produced by combustion of fossil fuels.

3.7 Statistical analyses

3.7.1 Correlation

A correlation table was created using the program PAST (Hammer et al., 2001) to assess the statistical relationships between all burial fluxes (BC, SCP and ACP), $CaCO_3$, organic matter (TOC, TN and TS), and heavy metals (Fe, Zn, Cu, Pb, As and Hg).

3.7.2 Principal component analysis

The data of all samples were summarized in a principal component analysis (PCA) to identify relationships among the measured parameters in the samples through time and regional distribution. The samples were centered and standardized by their variables (i.e. BC, SCP, ACP, OM and heavy metals) in a biplot of sample and species scores using the program C2 (Juggins, 2007). The sample of station DÖ-1 were excluded because of missing data of heavy metals. The simplification of the data might point out clusters of similar samples throughout this project or show a more random distribution of the samples.

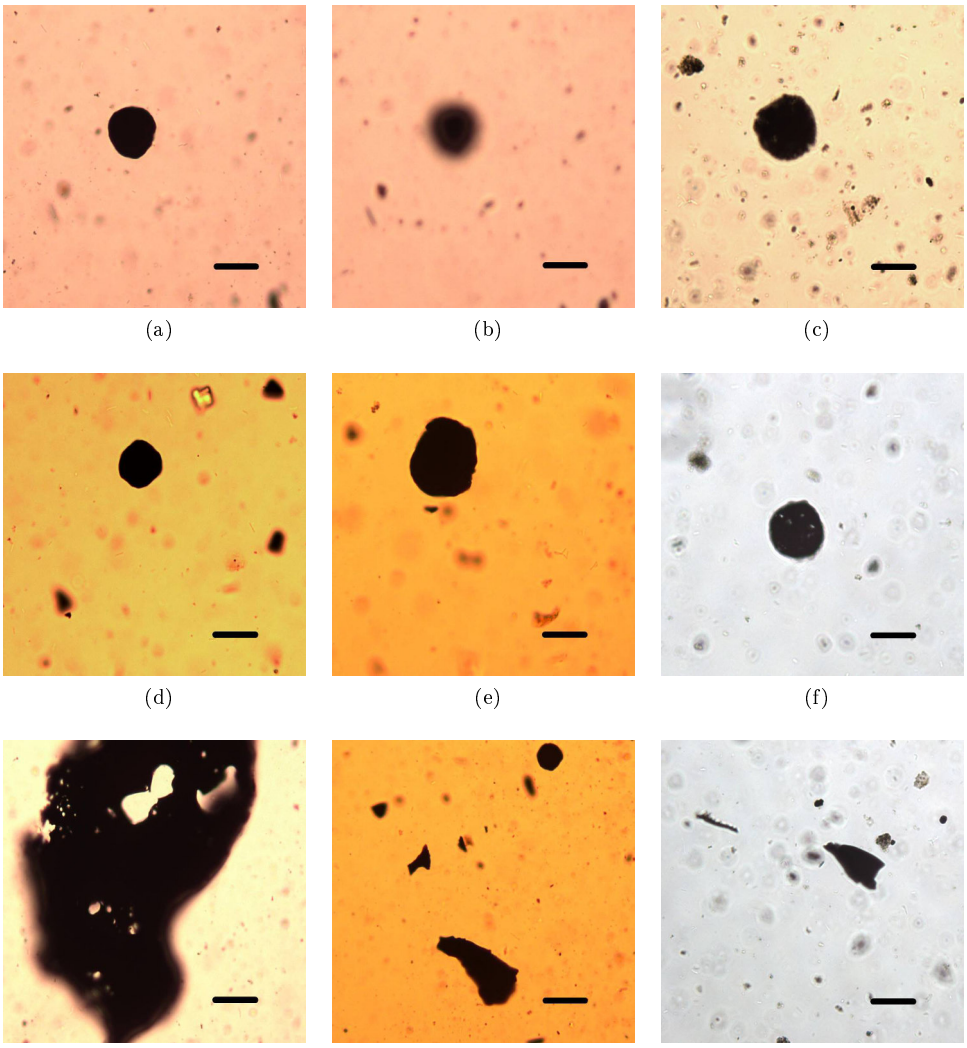

Figure 3: Speroidal (SCP; a - f) and amorphous carbonaceous particles (ACP; g - i) in the light microscope with a 200-fold magnification. Figure a and b show the spheroidal character of the SCP in different microscopic foci. The bar represents 25 µm.

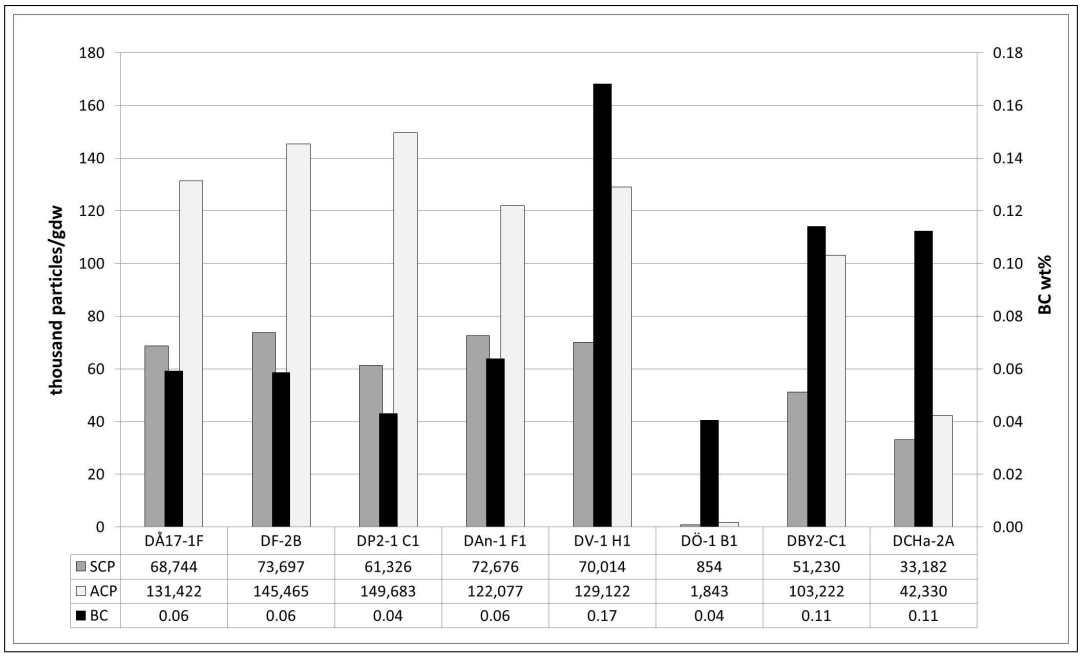

	DÅ17-1F	DF-2B	DP2-1 C1	DAn-1 F1	DV-1 H1	DÖ-1 B1	DBY2-C1	DCHa-2A
SCP	68,744	73,697	61,326	72,676	70,014	854	51,230	33,182
ACP	131,422	145,465	149,683	122,077	129,122	1,843	103,222	42,330
BC	0.06	0.06	0.04	0.06	0.17	0.04	0.11	0.11

Figure 4: Results of black carbon (BC), spheroidal and amorphous carbonaceous particles (SCP and ACP) of the samples from the station records off the south-west coast of Sweden.

4 Results

4.1 Surface samples off the Swedish south-west coast

4.1.1 Black carbon, spheroidal and amorphous carbonaceous particles

The BC concentrations from the Öresund are the highest (DV-1 H1: 0.17 wt%) and lowest (DÖ-1 B1: 0.04 wt%) of all surface samples (figure 4). The stations in the Arkona and Bornholm Sea (DBY2-C1 and DCHa-2A) show approximately twice as high values of 0.11 wt% compared to the stations from Skagerrak and Kattegat (0.04 - 0.06 wt %).

All stations show about twice as high abundances of ACP (2 - 150 thousand particles/gdw) than SCP (1 thousand - 74 thousand particles/gdw). Only the station in the Bornholm Sea (DCHa-2A) shows more equal particle numbers. DÖ-1 B1 in the Öresund has, in addition to the low BC concentration, also the lowest concentration of particles compared to the other stations. The stations in the Arkona Basin and Bornholm Sea show lower particle concentrations than the stations in the Skagerrak and Kattegat, in particular DCHa-2A (SCP/ACP: 33/42 thousand particles/gdw).

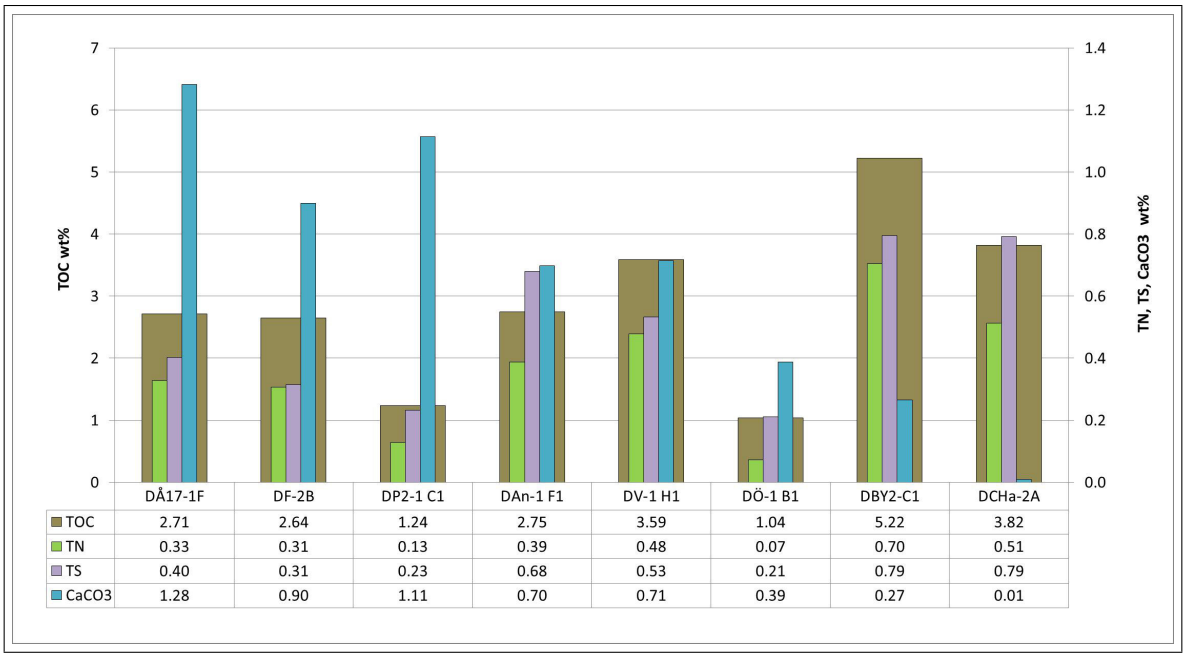

	DÅ17-1F	DF-2B	DP2-1 C1	DAn-1 F1	DV-1 H1	DÖ-1 B1	DBY2-C1	DCHa-2A
TOC	2.71	2.64	1.24	2.75	3.59	1.04	5.22	3.82
TN	0.33	0.31	0.13	0.39	0.48	0.07	0.70	0.51
TS	0.40	0.31	0.23	0.68	0.53	0.21	0.79	0.79
CaCO3	1.28	0.90	1.11	0.70	0.71	0.39	0.27	0.01

Figure 5: Results of organic matter and the calcium carbonate ($CaCO_3$) of the bottom surface samples from the stations off the Swedish south-west coast.

4.1.2 Organic matter

OM is most abundant in the Arkona Basin (DBY2-C1) followed by by the Bornholm Sea (DCHa-2A) and the Öresund (DV-1 H1; figure 5). The stations in the marine provinces Skagerrak and Kattegat further north show lower contents of OM. The samples DP2-1 C1 (Skagerrak) and DÖ-1 B1 (Öresund) show very low values in each fraction of OM. The content of $CaCO_3$ shows a declining trend from the north (1.28 wt%) to the south (0.01 wt%). The sample of the Gullmarn fjord has a slightly lower $CaCO_3$ value than the other two Skagerrak samples. TS (mean 0.44 wt%) is mostly more abundant than TN (mean: 0.36 wt%). The station DBY2-C1 in the Arkona Basin has the highest OM content; followed by DCHa-2A (Bornholm Sea) and DV-1 H1 in the Öresund. However, DAn-1 F1 shows a higher concentration of TS (0.68 wt%) than DV-1 H1 (0.53 wt%).

4.1.3 Heavy metals

The XRF scanning showed mostly the same pattern in abundances for heavy metals (figure 6). Sample DÖ-1 B1 was not available for the XRF scanning and is not included. Fe concentration had the largest range of all in the Skagerrak (DÅ17-1F, DF-2B and DP2-1 C1) between 2.05 - 3.12 wt% with an overall mean of 2.78 wt%. Zn concentrations showed a south-north gradient ranging from 99.21 mg/kg in the Bornholm Sea to 75.36 mg/kg in the Skagerrak except DP2-1 C1 (53.84 mg/kg). Pb concentrations were lowest in the

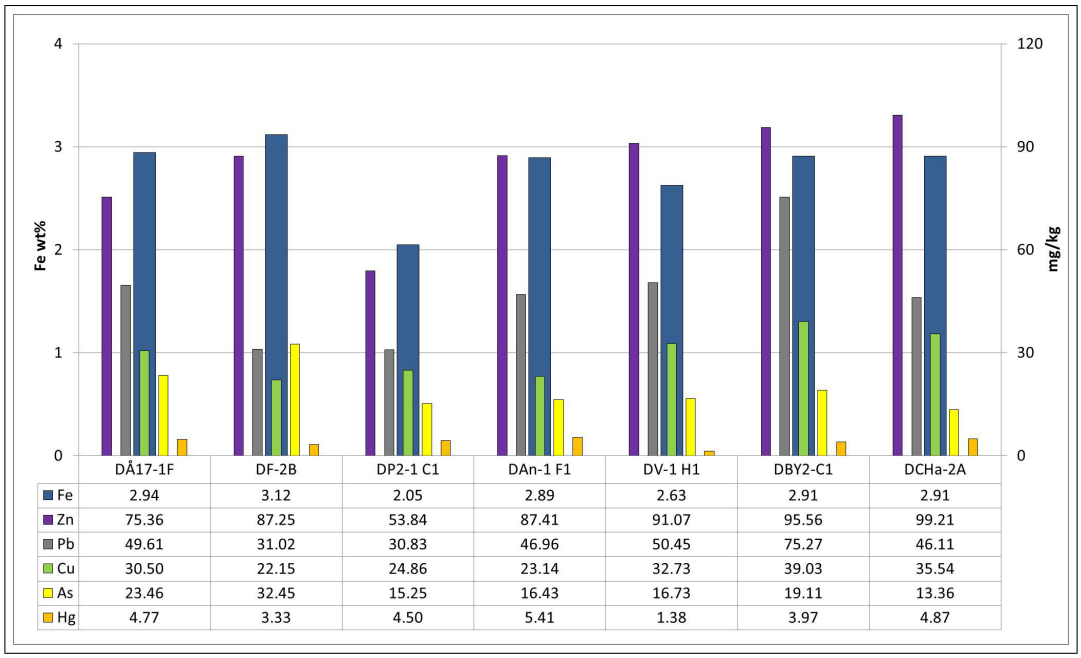

	DÅ17-1F	DF-2B	DP2-1 C1	DAn-1 F1	DV-1 H1	DBY2-C1	DCHa-2A
Fe	2.94	3.12	2.05	2.89	2.63	2.91	2.91
Zn	75.36	87.25	53.84	87.41	91.07	95.56	99.21
Pb	49.61	31.02	30.83	46.96	50.45	75.27	46.11
Cu	30.50	22.15	24.86	23.14	32.73	39.03	35.54
As	23.46	32.45	15.25	16.43	16.73	19.11	13.36
Hg	4.77	3.33	4.50	5.41	1.38	3.97	4.87

Figure 6: Results of heavy metals from the seafloor samples from the stations off the Swedish south-west coast.

two Skagerrak stations DF-2B and DP2-1 C1 (around 31 mg/kg) and had a mean of 47 mg/kg. The Pb concentration reached a high peak around 75 mg/kg in the Arkona Basin. Cu concentrations were highest in the Arkona Basin, Bornholm Sea and Öresund, respectively and had a similar pattern as Pb. However, the stations in the Skagerrak and Kattegat had the lowest Cu concentrations of all ranging between around 22 - 31 mg/kg. As was the only heavy metal that had the highest concentration around 32 mg/kg in the Gullmarn Fjord. It was the second highest abundant with about 23 mg/kg in the Skagerrak (DÅ17-1F). The Arkona Basin was the highest among the other stations, which varied between 13 - 19 mg/kg. The concentrations of Hg ranged between 1 - 5 mg/kg among all sampling statuions and were highest in the Kattegat. Öresund had the lowest concentration.

4.2 Sediment record from the Öresund strait

4.2.1 Age model and sedimentation rate

The decays of unsupported ^{210}Pb and ^{137}Cs show a downcore-decline in the G-core. Two peaks of unsupported ^{210}Pb-deacy appeared between 15 - 10 and 10 - 6 cm depth. The decay of ^{137}Cs showed a little increase in 16 - 15 cm depth and reached a peak between 9 - 8 cm depth which indicate the peaks of the nuclear bomb testing in 1963 and the catastrophe of Chernobyl in 1986 (green lines; figure 7).

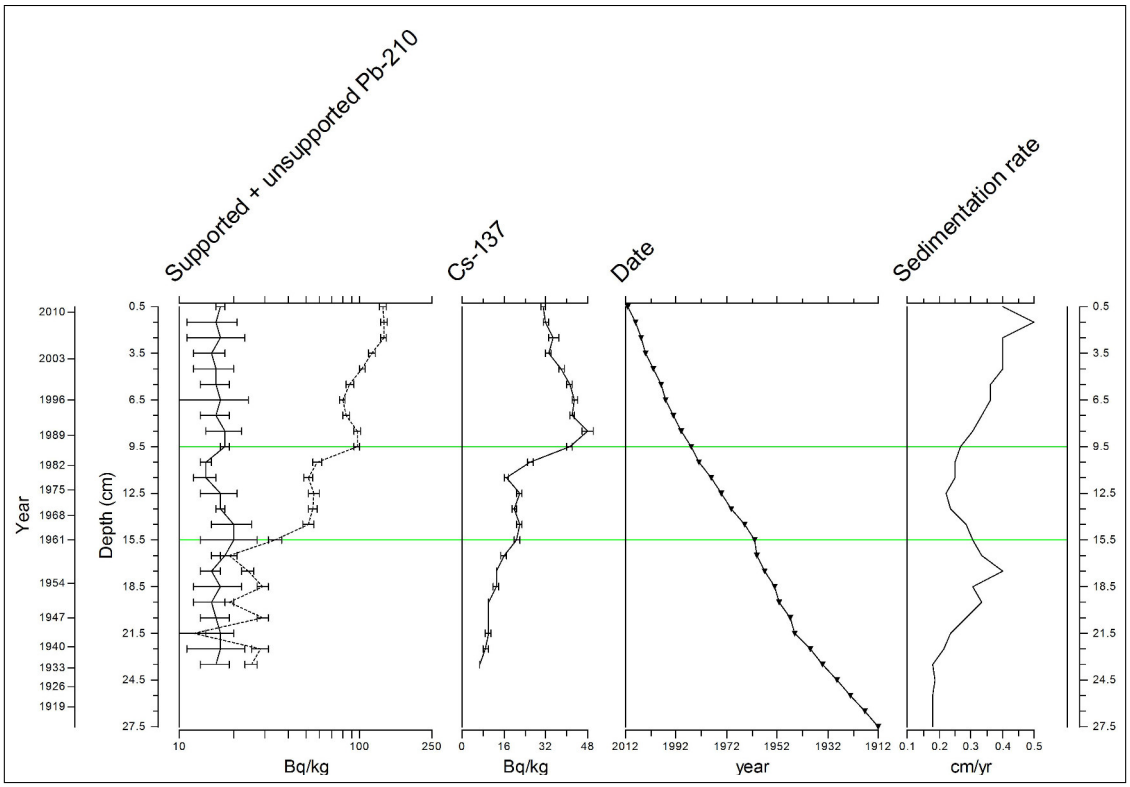

Figure 7: The age model, which is derived from unsupported ^{210}Pb (dashed line), was calibrated with^{137}Cs by Charrieau et al. (tted). The sedimentation rate was calculated from the age model. The green lines indicate the years of increased ^{137}Cs-increases due to atomic bomb tests and 1960 and the Chernobyl catastrophe in 1986.

Both radionuclides were used to create the age model, which ranges from 1912 to 2011. The sedimentation rate of the core was calculated using a running mean of five consecutive sedimentation rates (range: 0.18 - 0.5 cm/yr range; mean of 0.3 cm/yr) to smooth out high peaks (see figure 8a). The sedimentation rate of the lowermost part of core H (28 - 24 cm) has been extrapolated using the sedimentation rate of 0.18 cm/yr between 1934 and 1939 (24 - 22 cm). This extrapolation was used downcore using the two samples above for each time. The trend of the sedimentation rate reached the first high peak of 0.4 cm/yr in 1957 (18 - 17 cm depth). Afterwards the trend declined to a rate of 0.22 cm/yr until 1974 (13 - 12 cm depth). From then the trend climbed to its maximum peak of 0.5 cm/yr in 2008 (2 - 1 cm depth) and dropped slightly thereupon to 0.4 cm/yr in 2011.

4.2.2 Spheroidal and amorphous carbonaceous particles

The burial fluxes of BC, SCP and ACP were separated into two zones during which increasing fluxes can be observed. Zone I began after 1923 (orange line) and lasted until 1986 (figure 8a). The SCP burial flux reached a peak in Zone I with about 18,800 particles/cm^2/yr in 1957 and the ACP burial flux with about

19,000 particles/cm^2/yr in 1951. The SCP burial flux has smaller values from 1965 until 1986 and ranged between 4,400 - 9,500 particles/cm^2/yr. The ACP burial flux was more stable with a slightly negative trend until 1986.

In Zone II, a second phase became visible with an increase after 1986 and lasted until the end in 2011. During this second period, the particle burial fluxes showed an unproportionally high increase. The SCP burial flux reached the highest peak in 2008 with about 84,000 particles/cm^2/yr and the ACP burial flux with about 122,600 particles/cm^2/yr. Although SCP and ACP burial fluxes were closely correlated throughout the whole record, they also showed greater differences of their fluxes during the end of Zone I from 1965 until 1986 and Zone II between 1998 and 2004.

4.2.3 Black carbon and organic matter

The BC concentration at station DV-1 varied between 0.08 - 0.17 wt% with a mean of 0.11 wt%. In Zone I (figure 8a), the BC burial flux started to advance with about 36 µg/cm^2/yr in 1923 and ended with about 128 µg/cm^2/yr in 1986. During Zone I, the BC burial flux reached the highest peak about 379 µg/cm^2/yr in 1953 before the trend started to decline until 1986. The BC burial flux exhibited a significant drop in 1965 (blue line). At the end of the 1960s, OM started to decrease continuously and the concentrations of $CaCO_3$ (0.48 wt% in 1965) started to increase until the top of the record (0.71 wt% in 2011). The trends of the BC burial flux and OM declined until 1986 (red line). Only one sample with a BC burial flux of 368 µg/cm^2/yr in 1978 is significantly higher between 1965 and 1986. The beginning of Zone II started with the second increase of the BC burial flux in 1986 (red line) and the positive trend continued towards the top. The BC burial flux reached its overall maximum of 636 µg/cm^2/yr in 2008 and decreased slightly in 2011. TOC and TN showed a high content in 1996; TS in 1993. Between 1996 and 2008 (7 - 1 cm depth), the trends of TOC and TN dropped slightly and recovered again. Both ended up with high values above the mean of the record. The TS content decreased to its minimum in 2008 (2 - 1 cm depth) before it recovered slightly in 2011. The ratio of TOC/TN displayed a mostly marine signal of TOC (greater equal 10) with exceptions during the 1970s and 1990 when the ratio was above 10.

4.2.4 Heavy metals

The concentrations of Zn (52.4 - 62.0 mg/kg), Pb (26.3 - 32.8 mg/kg) and Cu (17.4 - 28.6 mg/kg) have their smallest concentrations throughout the whole record in the period from 1912 to 1960 (figure 8b). After 1960, all trends of the heavy metals except Fe increased. The concentrations of Fe dropped until 1983 and

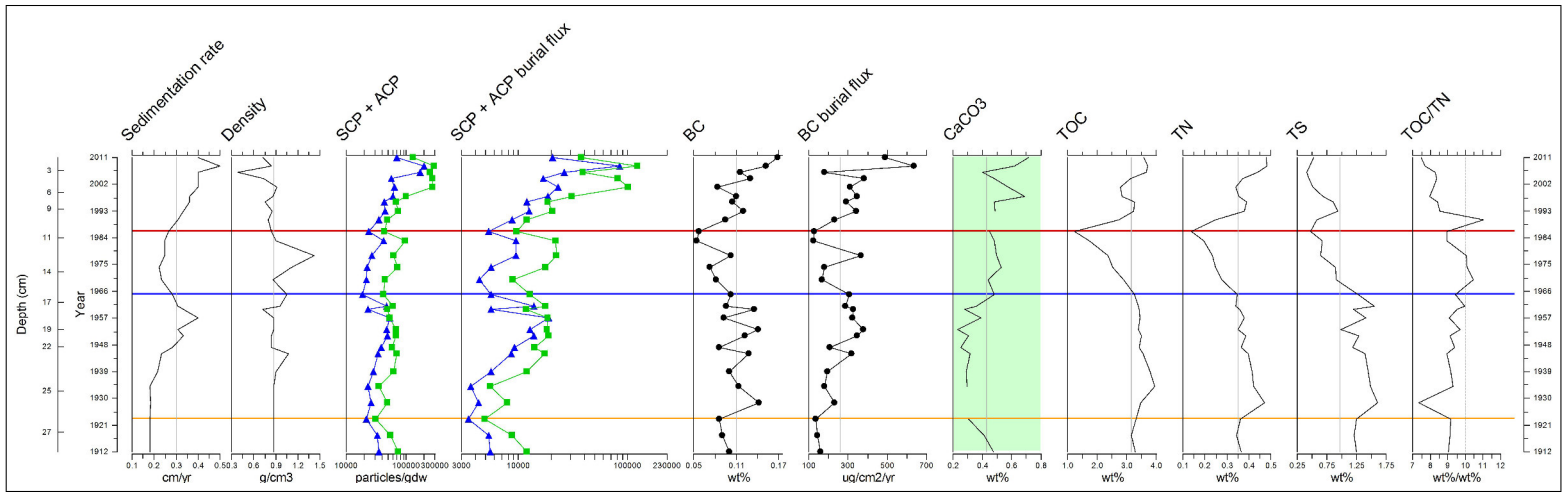

(a) The results of sedimentation rate, density, black carbon (BC), its burial flux, spheroidal (SCP; blue triangles), and amorphous carbonaceous particles (ACP; green squares), organic matter (i.e. total organic carbon (TOC), total nitrogen (TN), total sulfur (TS)) and TOC/TN ratio. The starting points of Zone I (orange line) in 1923 and Zone II (red line) in 1986 of combustion are shown. The change in BC and organic matter in 1965 (blue line) and the arithmetic means (vertical gray lines) are shown.

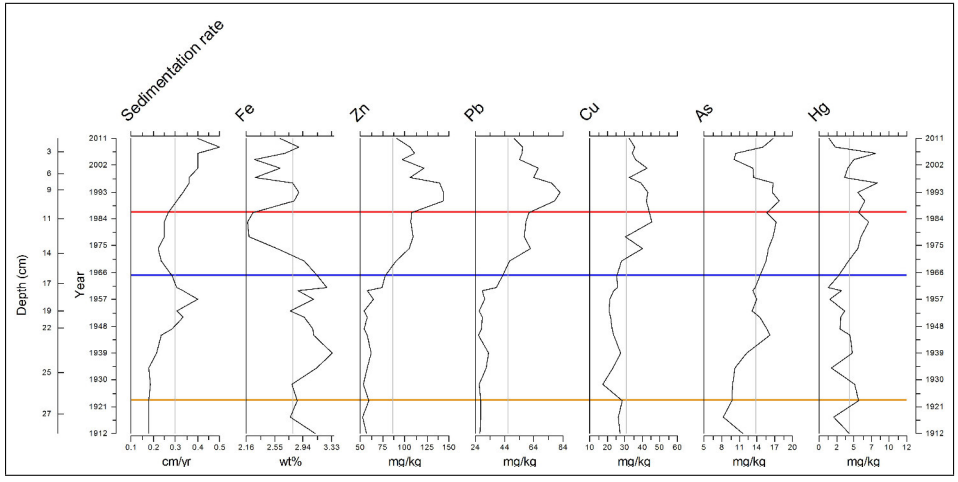

(b) The results of the sedimentation rate and heavy metals show a significant change during the beginning of the 1960s (blue line) resulting in a decrease of Fe and an increase of all other heavy metals (Zn, Pb, Cu, As, Hg). The starting points of Zone I (orange line) and Zone II (red line) of combustion and the arithmetic means (vertical gray lines) are shown.

Figure 8: Results of black carbon (BC), spheroidal and amorphous carbonaceous particles (SCP and ACP), organic matter and heavy metals from the Öresund record from 1912 - 2011.

recovered with a strong increase in 1986 to about 2.9 % in 1993. The Pb concentrations increased rapidly in 1986 and peaked at 82.0 mg/kg in 1993 (8 - 7 cm depth) before the trend decreased again until 2011. The Zn concentrations were almost twice as high as the Pb concentrations and with a similar trend as Cu, As and Hg. However, the concentrations of As (10.1 - 17.87 mg/kg) and Hg (1.4 - 8.0 mg/kg) vary strongly in the sediment after 1983. In the years 1974 until 1986, the concentrations of Zn (105.2 - 109.7 mg/kg) and Pb (57.4 - 61.7 mg/kg) stabilized. The trends of all heavy metals decreased after 1996 until the top of the record. Only As increased in 2011 again. Fe, Zn and Pb showed the same increase of concentrations between 1986 and 1998. The measurement of heavy metals had errors which are relative high for Cu, As and Hg.

4.3 Principal component analysis

A biplot of the PCA was created with the principle components (PC) 1 and 2, and the pollutants as eigenvectors (orange, half-filled circles; figure 9). PC 1 represents 38.0 % and PC 2 20.4 % of the variance in the data and explained 58.4 % of all variations of the data. For further simplification of the data, the samples were connected with two lines, which represent the chronological order for the Öresund record (dashed line) and in the north-south transect for the surface samples of 0 - 1 cm depth (solid line) from the Skagerrak (DÅ17-1F) to the Bornholm Sea (DCHa-2A). The surface sample DV-1 H1 represents the connection of the two lines. The samples from 1912 until 1965 are clustered which is mostly influenced by the eigenvectors of TS and Fe. The samples after 1965 and the 0 - 1 cm samples of the seafloor showed a more diffuse pattern and were identified as the second group. The samples 2006 and 2008 are strongly influenced by the very high variations of SCP and ACP and the samples after 1990 until 2004 were mostly controlled by the variations of the eigenvectors of Zn, Pb, Cu and Hg.

The burial fluxes of BC and SCP ($R^2 = 0.14$) and BC and ACP ($R^2 = 0.06$) were low correlated (table 2). The SCP and ACP burial fluxes have a high correlation of 0.7. All showed statistical significance to each other. The BC burial flux showed very low correlations with the heavy metals Fe, Zn and Pb ($R^2 \leq 0.08$), and no correlations with Cu, As and Hg ($R^2 = 0$). The ACP burial flux and the heavy metals Cu ($R^2 = 0.12$), Zn and Pb (both: $R^2 = 0.13$) showed low correlations. They were the strongest of all black carbon fractions. These three heavy metals showed the strongest correlations with each other of all (range of $R^2 = 0.71$ - 0.89) and are statistically significant. TS and Fe had a low correlation ($R^2 = 0.38$), which was statistically significant.

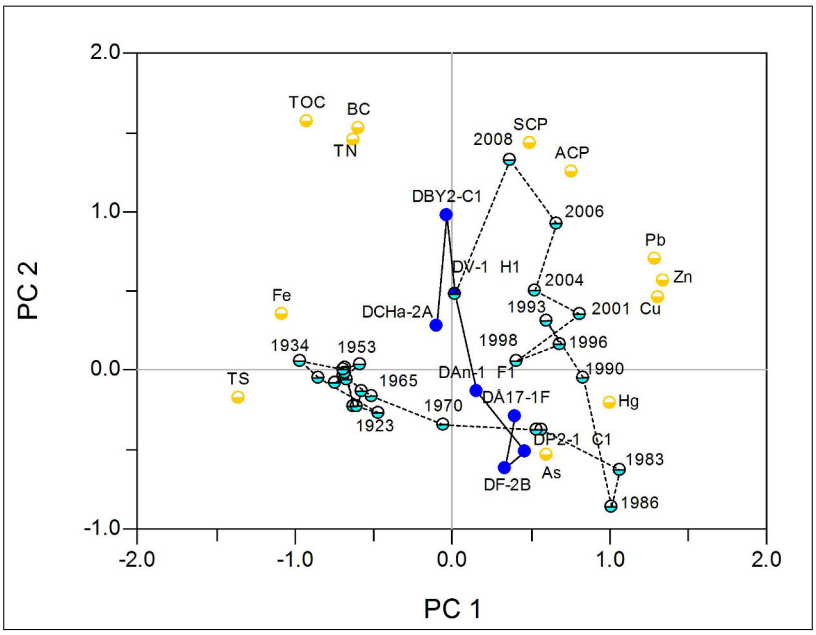

Figure 9: Principle component analysis of all samples and variables except the sample DÖ-1 B1. The eigenvalues for the principal component (PC) 1 is 38.0 %, and for PC 2 20.4 %. The light blue, half filled circles represent the samples (in years) of the Öresund record and are connected with a dashed line in chronological order. The dark blue circles represent the 0 - 1 cm surface samples, which are connected with a solid line in a north-south order from the Skagerrak (DÅ17-1F) to the Bornholm Sea (DCHa-2A). DV-1 H1 represents a surface sample as well as the year 2011 in the Öresund record.

Parameter	**Unit**	**0-1 cm depth at stations**		**Öresund record**	
		Range	**Mean**	**Range**	**Mean**
Sedimentation rate	cm/yr	-	-	0.18 - 0.50	0.30
Density	g/cm^3	-	-	0.39 - 1.43	0.87
BC	wt%	0.04 - 0.17	0.08	0.08 - 0.17	0.11
BC/TOC	wt%/wt%	2.18 - 4.68	2.99	2.52 - 4.68	3.42
BC burial flux	$\mu g/cm^2/yr$	-	-	33 - 636	301
SCP	particles/gdw	854 - 73,697	53,965	18,750 - 199,900	48,383
ACP		1,843 - 149,683	103,145	30,660 - 291,790	92,923
SCP burial flux	$particles/cm^2/yr$	-	-	900 - 83,960	12,625
ACP burial flux		-	-	1,270 - 122,550	24,729
$CaCO_3$	wt%	0.01 -1.28	0.67	0.23 - 0.71	0.43
TOC	wt%	1.04 - 5.22	2.88	1.25 - 3.94	3.15
TN		0.14 - 0.47	0.37	0.14 - 0.48	0.35
TS		0.21 - 0.79	0.49	0.41 - 1.60	0.98
TOC/TN	wt%/wt%	7.1 - 14.5	8.8	7.5 - 11.0	9.0
Fe	wt%	2.05 - 3.12	2.78	2.18 - 3.33	2.80
Zn	mg/kg	53.84 - 99.21	84.24	52.42 - 143.75	86.47
Pb		31.02 - 75.27	47.18	26.33 - 81.65	46.16
Cu		22.15 - 39.03	29.71	17.39 - 45.41	30.85
As		13.36 - 32.45	19.54	8.27 - 17.78	13.85
Hg		1.38 - 5.41	4.03	1.29 - 7.99	4.11

Table 1: Ranges and mean values of all samples separated in the stations and Öresund record.

	BC burial flux	SCP burial flux	ACP burial flux	$CaCO_3$	TOC	TN	TS	Fe	Zn	Cu	Pb	As	Hg
BC burial flux		0.050	0.039	0.241	0.246	0.242	0.054	0.151	0.266	0.777	0.268	0.852	0.970
SCP burial flux	0.14		0.000	0.031	0.250	0.123	0.031	0.886	0.191	0.349	0.227	0.619	0.259
ACP burial flux	0.06	0.70		0.006	0.685	0.343	0.002	0.252	0.062	0.066	0.065	0.933	0.510
$CaCO_3$	0.05	0.18	0.28		0.010	0.152	0.000	0.083	0.512	0.860	0.411	0.002	0.748
TOC	0.05	0.05	0.01	0.20		0.000	0.001	0.000	0.300	0.209	0.571	0.214	0.064
TN	0.23	0.09	0.04	0.07	0.58		0.055	0.137	0.227	0.415	0.817	0.031	0.387
TS	0.14	0.17	0.31	0.33	0.27	0.11		0.000	0.001	0.001	0.001	0.005	0.030
Fe	0.08	0.00	0.05	0.10	0.41	0.07	0.38		0.052	0.008	0.030	0.689	0.021
Zn	0.05	0.07	0.13	0.01	0.03	0.05	0.32	0.11		0.000	0.000	0.116	0.001
Cu	0.00	0.03	0.12	0.00	0.05	0.02	0.28	0.20	0.71		0.000	0.559	0.002
Pb	0.05	0.06	0.13	0.02	0.01	0.00	0.29	0.14	0.89	0.77		0.194	0.004
As	0.00	0.01	0.00	0.29	0.05	0.14	0.22	0.01	0.08	0.01	0.05		0.694
Hg	0.00	0.05	0.02	0.00	0.10	0.02	0.14	0.16	0.28	0.25	0.24	0.00	

Table 2: The correlation table shows R^2 in lower triangle and p-value in the upper one for the burial fluxes of black carbon, spheroidal and amorphous carbonaceous particles (SCP and ACP), and the contents of calcium carbonate ($CaCO_3$), organic matter (total organic carbon (TOC), total nitrogen (TN) and total sulfur (TS)), and heavy metals (Fe, Zn, Cu, Pb, As and Hg).

5 Discussion

5.1 Regional pollution patterns based on surface samples

Comparing BC, SCP and ACP, three separated types of combustion can be distinguished based on the geographic region which might be caused by different sources or processes. The first type results in low BC and high SCP and ACP in the marine provinces of Skagerrak and Kattegat. A second combustion type is in the Öresund which is high in BC and high in SCP and ACP (not considering DÖ-1 B1). The third combustion type is in the Arkona Basin and Bornholm Sea with high values of BC and lower SCP and ACP. The third type is similar to the second one of the Öresund but with lower concentrations of BC and SCP and ACP. The lower contents could be caused by a bigger sediment grain size in the Arkona Basin and Bornholm Sea. The lower concentrations of carbonaceous particles indicate that the marine provinces of the Öresund (DV-1 H1), Arkona Basin (DBY2-C1) and Bornholm Sea (DCHa-2a) are less polluted by fossil fuel combustion than the Skagerrak and Kattegat. However, the high BC concentrations of 0.11 - 0.17 wt% might be of a higher soot production.

The results of BC concentrations showed that the deposition is highest in the Öresund record (DV-1 H1: 0.17 wt%) and would indicated that the Öresund region is the one with the strongest pollution of the recent time. In contrast, the station DÖ-1, which is situated in close proximity to DV-1, showed the lowest BC content among all stations. A comparison of the grain sizes could improve our understanding about the stations' differences of the burial fluxes since small particles tend to bind to smaller grain sizes (muddy) rather than to greater ones (sandy). The complex Öresund's hydrography and sediment characteristics show that DV-1 is located in the lee of the island Ven and might have therefore a smaller grain size (muddy) than DÖ-1 (sandy) (Lumborg, 2005). This lee location could be the reason of pollutants as BC are more likely to deposit at DV-1.

Heavy metals showed no or low correlations with the burial fluxes of BC, SCP or ACP which suggests that fossil fuel combustion is not the main contributor of heavy metals to the coastal sediments off the south-west coast of Sweden. The higher concentrations of heavy metals in Arkona Basin (DBY2-C1) and Bornholm Sea (DCHa-2a) indicate a higher pollution due to heavy metals in the south compared to the other stations, located farther in the north. Although PC 1 and PC 2 only explained in total 58.4 % of the variances, the clustering showed that the the stations in the south (Öresund, DV-1 H1, except the excluded station DÖ-1; Arkona Basin, DBY2-C1; and Bornholm Sea, DCHa-2a) and in the north (Skagerrak, DÅ17-1F, DF-2B and DP2-1 C1; Kattegat, DAn-1 F1) were clustered in two groups which implied a distinct regional differences of pollution and a more polluted south.

One possible explanation of high values of TOC and TN at the stations of the Öresund, Arkona Basin and Bornholm Sea is a preservation of organic matter and can be related to anoxic or hypoxic conditions (Avramidis et al., 2014). The TOC/TN ratios were mostly below 10 with a mean of 7.9 and showed that the organic matter in the samples is derived by an autochthonous, algal source and not from terrestrial plants. Only DÖ-1 B1 from the Öresund showed a TOC/TN signal of 14.5 indicating significant contribution of organic matter derived from terrestrial plants. This signal showed that the two stations in the Öresund are exposed to different hydrographic processes, which could be an explanation for the lower contents of BC and OM in the sample of DÖ-1. Other explanations of the TOC and TN contents could be high sedimentation rates or high rates of primary production leading to high OM accumulation. The declining trend of $CaCO_3$ in the sediment samples from the Skagerrak in the north to the Bornholm Sea in the south might show a signal of a more marine Skagerrak and a more brackish Baltic Sea.

Sánchez-García et al. (2012) studied BC burial fluxes for the same marine provinces. In comparison with Sánchez-García et al. (2012), this study showed lower values of BC concentrations and burial fluxes in the Öresund for all the marine provinces (figure 10). One reason of this could be an oxidation of BC in this study during the CTO method that would lead to an underestimation of BC. This could for example happen if the temperature of the muffle furnace "overshoots" while heating up. Another explanation would be overestimation of the BC concentrations in Sánchez-García et al. (2012). The higher BC burial fluxes reported by Sánchez-García et al. (2012) might also be related to varying BC concentrations. The cause of these differences might be due to the chosen sample depth (0 - 2 cm vs. 0 - 1 cm in this study). In the Öresund record is shown that the sedimentation rate controls the BC concentration per depth significantly. Sánchez-García et al. (2012) assumed a mean sedimentation rate of 0.73 cm/yr which is almost twice as high compared to this study (DV-1 H1:ω = 0.4 cm/yr) and overall for the Öresund station DV-1 (mean ω = 0.3 cm/yr).

The assumed particle density of 2.5 g/cm^3 in Sánchez-García et al. (2012) and porosity of 0.75 (multiplied, it equals a factor of 0.625 g/cm^3) is lower than the density in the sample DV-1 H1 of the Öresund (ρ = 0.73 g/cm^3; mean ρ = 0.87). The high results of the CTO method and the high sedimentation rate in Sánchez-García et al. (2012) could have led to an overestimation and very high BC burial fluxes.

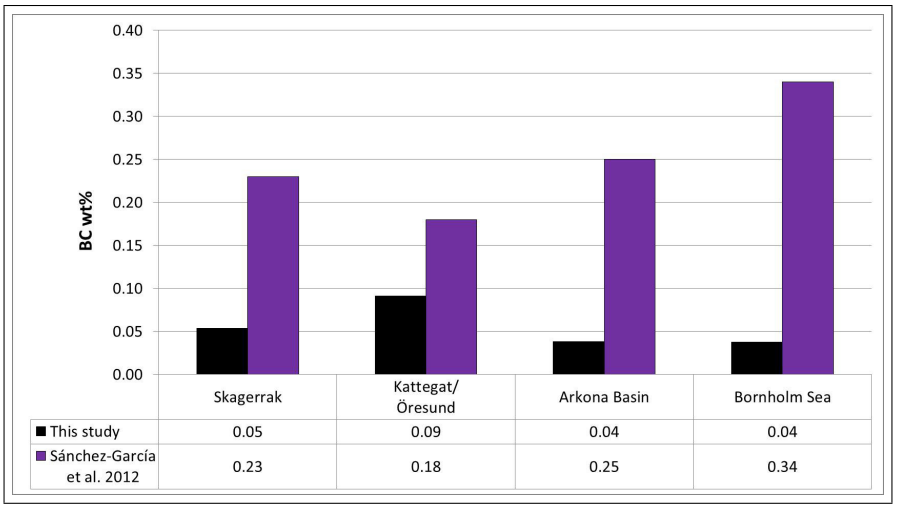

Figure 10: Means of black carbon (BC) compared with Sánchez-García et al. (2012) in the four marine provinces.

Marine Province		This study		Sánchez-García et al. 2012	
Skagerrak	BC (wt%)	0.04 - 0.06	n = 3	0.09 - 0.37	n = 8
	F_{burial} (µg/cm^2/yr)	-		398 - 1,963	
Kattegat/Öresund	BC (wt%)	0.04 - 0.17	n = 3	0.16 - 0.21	n = 13
	F_{burial} (µg/cm^2/yr)	491		727 - 960	
Arkona Basin	BC (wt%)	0.11	n = 1	0.18 - 0.33	n = 10
	F_{burial} (µg/cm^2/yr)	-		809 - 1,519	
Bornholm Sea	BC (wt%)	0.11	n = 1	0.14 - 0.53	n = 8
	F_{burial} (µg/cm^2/yr)	-		661 - 2,427	

Table 3: Ranges of black carbon (BC) and its burial flux compared with Sánchez-García et al. (2012).

5.2 Öresund record

5.2.1 Age model and sedimentation rate

The age model was created by the calibration of ^{210}Pb and ^{137}Cs. The deposition of ^{210}Pb was affected by varying concentrations of ^{210}Pb which were washed out from the atmosphere, events of turbation and erosion, and unsteady sedimentation rates of the Öresund. In particular, the two plateaus of unsupported ^{210}Pb appeared between 15 - 10 and 10 - 6 cm depth might indicate turbation events. These uncertainties might have caused errors in the age model and affected the calculation of the sedimentation rate.

The sedimentation rate played a key role as physical factor in the contribution to the burial fluxes of BC, SCP and ACP. High peaks of the sedimentation rate led as well to high peaks in the burial fluxes and vice versa. The samples below a depth of 24 cm had the greatest uncertainty referring to the sedimentation rate because of the downcore extrapolation.

5.2.2 Combustion history

A reason for the drop in the BC burial flux during the 1960s lasting until 1980s could be due to an improvement of air quality as a positive effect of several legislative actions. Coal and coke were replaced by oil and the legislative policies targeted the diminution of emissions as adoption of pollution controls of coal-fired power plants and traffic exhaust (Elmquist et al., 2007; Libes, 2009). The 1970s were a continuation of those air pollution controls, going alongside with the shutdown of some heavily polluting factories (Anderberg, 2009). The area underwent an investment in district heating, which led to a decrease of fossil fuel-based heating (Anderberg, 2009). Anderberg (2009) stated that Copenhagen's (96 %) and Malmö's apartment buildings (90 %) receive their heating from remote networks. These circumstances could be an explanation for the lower burial fluxes of BC after 1965. That saying, the traffic pollution can be assumed to be the main source up-to-date and responsible for the large increase of fossil fuel consumption in Zone II as it is potentially produced in shipping exhaust. Bond et al. (2013) stated that around 2 % of global BC emissions is contributed by marine shipping. Additionally, road traffic increased since the opening of the Öresund Bridge in 2000. However, the SCP burial flux implied that the emitting source is mainly increasing ship and car traffic since the late 1980s and might show an evidence of a increased usage of cars and shipping in the Öresund region. The heavy metals showed no or low correlations to the burial fluxes of BC, SCP and ACP, which indicates different main sources of heavy metals than fossil fuel combustion in the Öresund record. With perspective to the combustion history of the Öresund region, this study concluded that the peaks of the BC, SCP and ACP burial fluxes indicate a strong contribution of house heating before the legislative actions against air pollution in 1960s and enhanced shipping in the Öresund strait since 1993.

In a study by Elmquist et al. (2007) BC burial fluxes were investigated in lake sediment records, which was collected near the EMEP Air Monitoring Station in Aspvreten (70 km south of Stockholm, south-east Sweden) and was dated up to 2005 (figure 11). They found the highest BC burial flux in 1928 (40 µg/cm^2/yr) and a second peak about 33 µg/cm^2/yr in 1960. During the beginning of the 1920s, the BC burial fluxes of about 36 - 64 µg/cm^2/yr of this study are similar to Elmquist et al. (2007) in the beginning of the 1920s but start to increase in the end of the 1920s (start of Zone I). However, in this study the highest BC burial flux of about 636 µg/cm^2/yr was estimated for 2008 and is more than 127-fold compared to the estimated BC burial flux of about 5 µg/cm^2/yr in 2007 by Elmquist et al. (2007). This difference in the burial fluxes is most likely due to the different air pollution in the regions. The study by Elmquist et al. (2007) and this one show different trends of the BC burial fluxes and, thus, were likely affected by different, regional combustion sources or processes. However, the large drop after 1965 (blue line) is also notable by the clustering in the PCA and by a decline of the burial flux in Elmquist et al. (2007) but which is not that rapid. These patterns

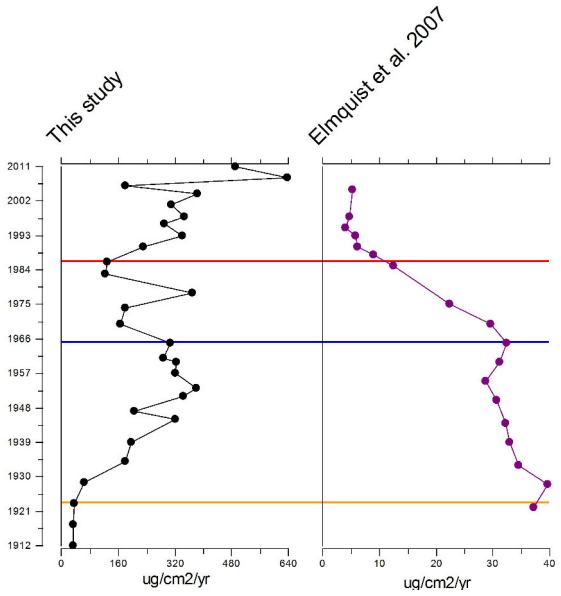

Figure 11: Black carbon (BC) burial flux compared with Elmquist et al. (2007).

in the trends of both studies emphasizes the assumption that the air quality improved as a positive effect of several legislative actions but in different extents and imply a matching chronology for this time.

As shown above in the regional distribution of BC, SCP and ACP concentrations, the unequal patterns of the BC, SCP and ACP burial fluxes leads as well to the assumption that the ratios of the burial fluxes indicate changes of the main sources and processes of combustion during in the last century. Research on their ratios could reveal patterns for these sources and processes.

5.2.3 Oxidation of BC?

The decline in BC burial flux between 1965-1985 can be explained two ways. Firstly, the record indicated that the BC burial flux dropped as a consequence of the air pollution policies in the beginning of the 1960s. However, during that time a recognizable low burial event of OM and the Fe as well as a higher abundance of $CaCO_3$ appeared in the record. The same trends of TS and Fe might indicate the abundance of pyrite (FeS). Further analysis of pyrite in the sediment record could strengthen this argument (Avramidis et al., 2014). Those proxies for environmental conditions imply an oxidation event that could be caused by a change in the the complex hydrography of the Öresund Lumborg (2005). This change could either bring more oxic bottom water and - with that - more biological activity.

The increase of $CaCO_3$ and, thus, biological activity implies a remineralization of OM in oxic bottom waters (dissolved oxygen content: $>$ 2 mL/L) after the dropping event between the mid 1960s until 1990s. The

scarcity of $CaCO_3$ and high accumulation of OM before 1965 pointed to a rather low biological activity and higher OM preservation in hypoxia or anoxia, which was perhaps caused by eutrophication (Lumborg, 2005).

Secondly, this change of oxic conditions at the sediment surface might have contributed as well to a possible BC degradation due to remineralization during the time of BC burial. Hartnett et al. (1998), Middelburg et al. (1999), Moodley et al. (2005) and Middelburg & Levin (2009) found that the oxygen exposure time has an impact on the carbon preservation and Middelburg et al. (1999) found that BC degrades in marine sediments when exposed to oxygen (and nitrate) but pointing out that the involved microbiological and chemical mechanisms are not understood yet. However, Goldberg (1985) suggested that microbiological and chemical mechanisms are the primary processes of BC degradation. Parsons et al. (2007) partly answered this gap of knowledge showing that BC is bioavailable as an very important geosorbent with respect to sorption when phenanthrene (PHE), a polycyclic armomatic hydrocarbon (PAH), is low in its concentrations (ng/L and below). Those findings suggest the hypothesis that this study showed a BC degradation in an oxic environment after 1965 since the TOC and BC dropped in the sedimentary record. That would suggest an underestimation of the burial flux of the as recalcitrant known BC in the record.

6 Conclusion

This study analyzed the spatial and temporal patterns of pollution, deposited in coastal sediments of south-west Sweden. The reconstructed burial fluxes of BC, SCP and ACP (or charcoal) were related to the history of (fossil fuel) combustion. The burial fluxes of BC, SCP and ACP showed that the highest contamination due to combustion processes was after 1945 until 1965 and 1993 until 2011.

Although the legislative actions were applied in the beginning of the 1960s, the trend of the BC burial flux only declined from 1960s until 1980s and showed a strongly positive trend after 1986. Heavy metals and the burial fluxes of BC, SCP and ACP did not show any similarities even though they have a common source with the combustion of fossil fuel. Therefore, there had to be other main sources than combustion for heavy metals in the coastal sediments of south-west Sweden. The BC, SCP and ACP burial fluxes in this study indicate a strong contribution of house heating before the legislative actions against air pollution in 1960s and enhanced shipping in the Öresund strait since 1993

The heavy metals Zn, Pb, Cu, As and Hg (all except Fe) are similar in their depositional trends signaling that they might have been emitted from the same sources and/or processes, which started to increase during the begin of the 1960s. All heavy metals might have been influenced by the same redox processes in the sediment as well. However, they did not show strong similarities to any of the burial fluxes which implied that combustion of fossil fuel was no main source of them.

The fractions of black carbon are known to be recalcitrant and not easily degradable. However, the BC burial flux exhibited a similar decrease as OM and Fe concentrations (similar trends of TS and Fe maybe indicate FeS) between the 1960s and 1990s. The environmental conditions off the Swedish south-west coast and for the period from 1912 until 2011 in Öresund record using organic matter and heavy metals, which are reactive depending on the oxygen concentration of the bottom-water. The trends of OM (i.e. TOC, TN and TS) showed strong similarities of preservation and were identified as possible proxies for the oxygen content of the bottom water.

6.1 Future research

As many questions need to be answered coming up with this project, future research could be applied on many diverse matters following up on this study as well as in more general approaches. A first step for further research might be a comparison of the ratios of burial fluxes of the BC, SCP and ACP. This comparison of ratios might show patterns about their sources of production assuming that traffic exhaust is the main

source of the ratio nowadays. Grain size analysis need to be applied for the future as small compounds as BC and heavy metals are rather buried in smaller grain sizes as mud. It is a key factor of sedimentation of pollution in coastal sediments (Lumborg, 2005).

Another approach to improve the understanding of BC burial in the Öresund region is comparing the BC burial flux with records of BC burial fluxes from lake or fjord sediments with more stable sedimentation rates from the same area as a control record. This comparison with another sedimentary record might verify the quantification of the BC burial flux in coastal sediments of the Öresund. To see how much BC is actually buried of the total BC production, the estimation of BC fraction with 1-3 % to total C production during the combustion process by Druffel (2004) could be applied for calculations. This approach could show the differences of the BC burial flux and the BC production and might lead to questions about the pathways of possibly missing BC.

To further study the question whether a real pollution history is represented in the record, a sounder understanding of the circumstances of BC degradation (Goldberg, 1985; Masiello, 2004) is necessary since this study point out the possibility of BC degradation in oxic bottom water conditions (Middelburg et al., 1999). For instance, a long-term observation program with five- or ten-year intervals with coring or sediment traps in aquatic environments with different conditions (e.g. anoxic, hypoxic, oxic, acidic etc.), and photochemical experiments could be performed. Various fractions of black carbon have their own recalcitrant characteristics and might be differently bioavailable. Investigations on the concentrations of PHE could contribute to the understanding of bioavailability/sorption of BC and shrink the underestimation of BC in the increasingly oxygenated time since 1960s. This could imply as well whether BC and SCP in coastal sediments could be a reliable dating tool for the Anthropocene (see Rose, 2015).

A study about ACP with electron microscopy could identify the particles' identity and whether it is actually charcoal. Pyrite could be investigated as well with this method and could serve as a proxy for hypoxic conditions. Furthermore, SCP and ACP could be investigated for their content of heavy metals. If they are abundant enough for applying the method of magnetic susceptibility, this could possibly be developed as a low prized control-proxy for heavy metals containing SCP/ACP (see Thevenon & Anselmetti, 2007). The ratio of inorganic fly-ash particles (IAS) to SCP could be applied to establish the point of change of fossil fuels from coal to oil (see Bond et al., 2013).

References

Adriano, D. C. (2001). *Trace Elements in Terrestrial Environments*. Springer Nature.

Anderberg, S. (2009). *Transcending boundaries. Environmental histories from the Øresund Region*, chapter Industrialization and environmental development around the Øresund - A long-term perspective on the regional development, (pp. 52–74). Skrifter med Historiska Perspektiv, Malmö högskola, 9 edition.

Appleby, P. G. (2001). *Chronostratigraphic Techniques in Recent Sediments*, (pp. 171–203). Springer Netherlands: Dordrecht.

Appleby, P. G. & Oldfieldz, F. (1983). The assessment of 210Pb data from sites with varying sediment accumulation rates. *Hydrobiologia*, 103(1), 29–35.

Avramidis, P., Iliopoulos, G., Panagiotaras, D., Papoulis, D., Lambropoulou, P., Kontopoulos, N., Siavalas, G., & Christanis, K. (2014). Tracking mid- to late holocene depositional environments by applying sedimentological, palaeontological and geochemical proxies, amvrakikos coastal lagoon sediments, western Greece, mediterranean sea. *Quaternary International*, 332, 19–36.

Bond, T. C., Doherty, S. J., Fahey, D. W., Forster, P. M., Berntsen, T., DeAngelo, B. J., Flanner, M. G., Ghan, S., Kärcher, B., Koch, D., Kinne, S., Kondo, Y., Quinn, P. K., Sarofim, M. C., Schultz, M. G., Schulz, M., Venkataraman, C., Zhang, H., Zhang, S., Bellouin, N., Guttikunda, S. K., Hopke, P. K., Jacobson, M. Z., Kaiser, J. W., Klimont, Z., Lohmann, U., Schwarz, J. P., Shindell, D., Storelvmo, T., Warren, S. G., & Zender, C. S. (2013). Bounding the role of black carbon in the climate system: A scientific assessment. *Journal of Geophysical Research: Atmospheres*, 118(11), 5380–5552.

Bryan, G. & Langston, W. (1992). Bioavailability, accumulation and effects of heavy metals in sediments with special reference to United Kingdom estuaries: a review. *Environmental Pollution*, 76(2), 89–131.

Callender, E. (2014). 11.3 - heavy metals in the environment - historical trends. In H. D. Holland & K. K. Turekian (Eds.), *Treatise on Geochemistry (Second Edition)* (pp. 59 – 89). Oxford: Elsevier, second edition edition.

Carbone, S., Onasch, T., Saarikoski, S., Timonen, H., Saarnio, K., Sueper, D., Rönkkö, T., Pirjola, L., Häyrinen, A., Worsnop, D., & Hillamo, R. (2015). Characterization of trace metals on soot aerosol particles with the SP-AMS: detection and quantification. *Atmos. Meas. Tech.*, 8(11), 4803–4815.

Charrieau, L. M., H. L. Filipsson, K. Ljung, M. C., Knudsen, K. L., & Kritzberg, E. (submitted). The effects of multiple stressors on the distribution of coastal benthic foraminifera: a case study from the skagerrak-baltic sea region. *Limnology and Oceanography*.

Chung, C. E., Ramanathan, V., Kim, D., & Podgorny, I. A. (2005). Global anthropogenic aerosol direct forcing derived from satellite and ground-based observations. *J. Geophys. Res.*, 110(D24).

Chung, S. H. & Seinfeld, J. H. (2002). Global distribution and climate forcing of carbonaceous aerosols. *Journal of Geophysical Research: Atmospheres*, 107(D19), AAC 14–1–AAC 14–33. 4407.

Cutshall, N. H., Larsen, I. L., & Olsen, C. R. (1983). Direct analysis of 210Pb in sediment samples: Self-absorption corrections. *Nuclear Instruments and Methods in Physics Research*, 206(1-2), 309–312.

Danielsson, Å., Cato, I., Carman, R., & Rahm, L. (1999). Spatial clustering of metals in the sediments of the Skagerrak/Kattegat. *Applied Geochemistry*, 14(6), 689–706.

Dave, G. & Dennegård, B. (1994). Sediment toxicity and heavy metals in the Kattegat and Skaggerak. *Journal of Aquatic Ecosystem Health*, 3(3), 207–219.

Druffel, E. R. (2004). Comments on the importance of black carbon in the global carbon cycle. *Marine Chemistry*, 92(1-4), 197–200.

Elmquist, M., Cornelissen, G., Kukulska, Z., & Gustafsson, Ö. (2006). Distinct oxidative stabilities of char versus soot black carbon: Implications for quantification and environmental recalcitrance. *Global Biogeochemical Cycles*, 20(2), n/a–n/a.

Elmquist, M., Gustafsson, Ö., & Andersson, P. (2004). Quantification of sedimentary black carbon using the chemothermal oxidation method: an evaluation of ex situ pretreatments and standard additions approaches. *Limnology and Oceanography: Methods*, 2(12), 417–427.

Elmquist, M., Zencak, Z., & Gustafsson, Ö. (2007). A 700 year sediment record of black carbon and polycyclic aromatic hydrocarbons near the EMEP air monitoring station in Aspvreten, Sweden. *Environmental Science and Technology*, 41, 6926.

Forbes, M., Raison, R., & Skjemstad, J. (2006). Formation, transformation and transport of black carbon (charcoal) in terrestrial and aquatic ecosystems. *Science of The Total Environment*, 370(1), 190–206.

Förstner, U. & Wittmann, G. T. W. (1981). *Metal Pollution in the Aquatic Environment*. Springer Science Business Media.

Goldberg, E. (1985). *Black carbon in the environment*. Wiley and Sons,New York, NY.

Gustafsson, Ö., Bucheli, T. D., Kukulska, Z., Andersson, M., Largeau, C., Rouzaud, J.-N., Reddy, C. M., & Eglinton, T. I. (2001). Evaluation of a protocol for the quantification of black carbon in sediments. *Global Biogeochemical Cycles*, 15(4), 881–890.

Gustafsson, Ö. & Gschwend, P. M. (1998). The flux of black carbon to surface sediments on the New England Continental Shelf. *Geochimica et Cosmochimica Acta*, 62(3), 465 – 472.

Hammer, Ø., Harper, D. A. T., & Ryan, P. (2001). Past: Paleontological statistics software package for education and data analysis. *Palaeontologia Electronica*, 4(1), 9pp.

Hammes, K., Schmidt, M. W. I., Smernik, R. J., Currie, L. A., Ball, W. P., Nguyen, T. H., Louchouarn, P., Houel, S., Gustafsson, Ö., Elmquist, M., Cornelissen, G., Skjemstad, J. O., Masiello, C. A., Song,

J., Peng, P., Mitra, S., Dunn, J. C., Hatcher, P. G., Hockaday, W. C., Smith, D. M., Hartkopf-Fröder, C., Böhmer, A., LÃŒer, B., Huebert, B. J., Amelung, W., Brodowski, S., Huang, L., Zhang, W., Gschwend, P. M., Flores-Cervantes, D. X., Largeau, C., Rouzaud, J.-N., Rumpel, C., Guggenberger, G., Kaiser, K., Rodionov, A., Gonzalez-Vila, F. J., Gonzalez-Perez, J. A., de la Rosa, J. M., Manning, D. A. C., López-Capél, E., & Ding, L. (2007). Comparison of quantification methods to measure fire-derived (black/elemental) carbon in soils and sediments using reference materials from soil, water, sediment and the atmosphere. *Global Biogeochemical Cycles*, 21(3).

Hartnett, H. E., Keil, R. G., Hedges, J. I., & Devol, A. H. (1998). Influence of oxygen exposure time on organic carbon preservation in continental margin sediments. *Nature*, 391(6667), 572–575.

Hedges, J., Eglinton, G., Hatcher, P., Kirchman, D., Arnosti, C., Derenne, S., Evershed, R., Kögel-Knabner, I., de Leeuw, J., Littke, R., Michaelis, W., & Rullkötter, J. (2000). The molecularly-uncharacterized component of nonliving organic matter in natural environments. *Organic Geochemistry*, 31(10), 945–958.

IPCC (2013). *Climate Change 2013: The Physical Science Basis. Contribution of Working Group I to the Fifth Assessment Report of the Intergovernmental Panel on Climate Change*. Cambridge, United Kingdom and New York, NY, USA: Cambridge University Press.

Juggins, S. (2007). *C2 Version 1.5 User guide. Software for ecological and palaeoecological data analysis and visualisation*. Newcastle University, Newcastle upon Tyne, UK.

Li, S.-L., Calmels, D., Han, G., Gaillardet, J., & Liu, C.-Q. (2008). Sulfuric acid as an agent of carbonate weathering constrained by δ13Cdic: Examples from southwest China. *Earth and Planetary Science Letters*, 270(3-4), 189–199.

Libes, S. (2009). *Introduction to Marine Biogeochemistry*. Academic Press, 2nd edition.

Lintrup, M. & Jakobsen, F. (1999). The importance of öresund and the drogden sill for baltic inflow. *Journal of Marine Systems*, 18(4), 345–354.

Lippmann, M. & Albert, R. E. (1969). The effect of particle size on the regional deposition of inhaled aerosols in the human respiratory tract. *American Industrial Hygiene Association Journal*, 30(3), 257–275.

Lumborg, U. (2005). Modelling the deposition, erosion, and flux of cohesive sediment through Øresund. *Journal of Marine Systems*, 56(1-2), 179–193.

Mannino, A. & Harvey, H. R. (2004). Black carbon in estuarine and coastal ocean dissolved organic matter. *Limnol. Oceanogr.*, 49(3), 735–740.

Masiello, C. A. (2004). New directions in black carbon organic geochemistry. *Marine Chemistry*, 92(1), 201–213.

Mejía-Piña, K. G., Huerta-Diaz, M. A., & González-Yajimovich, O. (2016). Calibration of handheld x-ray fluorescence (XRF) equipment for optimum determination of elemental concentrations in sediment samples. *Talanta*, 161, 359–367.

Middelburg, J. J. & Levin, L. A. (2009). Coastal hypoxia and sediment biogeochemistry. *Biogeosciences*, 6(7), 1273–1293.

Middelburg, J. J., Nieuwenhuize, J., & van Breugel, P. (1999). Black carbon in marine sediments. *Marine Chemistry*, 65(3-4), 245–252.

Moodley, L., Middelburg, J. J., Herman, P. M., Soetaert, K., & de Lange, G. J. (2005). Oxygenation and organic-matter preservation in marine sediments: Direct experimental evidence from ancient organic carbon–rich deposits. *Geology*, 33(11), 889.

Oberdörster, G. & Yu, C. (1990). Proceedings of the 1990 european aerosol conference the carcinogenic potential of inhaled diesel exhaust: a particle effect? *Journal of Aerosol Science*, 21, S397 – S401.

Parsons, J., Segarra, M. J. B., Cornelissen, G., Gustafsson, Ö., Grotenhuis, T., Harms, H., Janssen, C. R., Kukkonen, J., van Noort, P., Calvo, J. J. O., & Etxeberria, O. S. (2007). Characterisation of contaminants in sediments - effects of bioavailability on impact. In D. Barceló & M. Petrovic (Eds.), *Sediment Quality and Impact Assessment of Pollutants*, volume 1 of *Sustainable Management of Sediment Resources* (pp. 35 – 60). Elsevier.

Rae, J. (1997). *Biogeochemistry of intertidal sediments*, chapter Trace metals in deposited intertidal sediments, (pp. 16 – 41). Cambridge University Press, Cambridge.

Ramanathan, V. & Carmichael, G. (2008). Global and regional climate changes due to black carbon. *Nature Geoscience*, 1(4), 221–227.

Renberg, I., Korsman, T., & Anderson, N. J. (1993). A Temporal Perspective of Lake Acidification in Sweden. *Ambio*, 22(5), 264–271.

Rose, N. (1990). A method for the extraction of carbonaceous particles from lake sediment. *Journal of Paleolimnology*, 3(1), 45–53.

Rose, N. & Juggins, S. (1994). A spatial relationship between carbonaceous particles in lake sediments and sulphur deposition. *Atmospheric Environment*, 28(2), 177–183.

Rose, N. L. (1994). A note on further refinements to a procedure for the extraction of carbonaceous fly-ash particles from sediments. *Journal of Paleolimnology*, 11, 201.

Rose, N. L. (2015). Spheroidal carbonaceous fly-ash particles provide a globally synchronous stratigraphic marker for the Anthropocene. *Environmental Science and Technology*, 49, 4155.

Rose, N. L. & Ruppel, M. (2015). Environmental archives of contaminant particles. In *Environmental Contaminants* (pp. 187–221). Springer Netherlands.

Rosenberg, R., Cato, I., Förlin, L., Grip, K., & Rodhe, J. (1996). Marine environment quality assessment of the Skagerrak - Kattegat. *Journal of Sea Research*, 35(1-3), 1–8.

Ruppel, M. M. (2015). *Black carbon deposition in the European Arctic from the preindustrial to the present.* PhD thesis, University of Helsinki, Faculty of Biological and Environmental Sciences, Department of Environmental Sciences, Environmental Change Research Unit. Doctoral dissertation (article-based).

Ruppel, M. M., Gustafsson, Ö., Rose, N. L., Pesonen, A., Yang, H., Weckström, J., Palonen, V., Oinonen, M. J., & Korhola, A. (2015). Spatial and temporal patterns in black carbon deposition to dated Fennoscandian Arctic lake sediments from 1830 to 2010. *Environmental Science & Technology*, 49(24), 13954–13963. PMID: 26575216.

Sánchez-García, L., Cato, I., & Gustafsson, Ö. (2012). The sequestration sink of soot black carbon in the Northern European Shelf sediments. *Global Biogeochemical Cycles*, 26(1).

Sanderson, M. G., Collins, W. J., Johnson, C. E., & Derwent, R. G. (2006). Present and future acid deposition to ecosystems: The effect of climate change. *Atmospheric Environment*, 40(7), 1275 – 1283.

Sayin, E. & Krauss, W. (1996). A numerical study of the water exchange through the danish straits. *Tellus A*, 48(2), 324–341.

Smith, S. J., Pitcher, H., & Wigley, T. (2001). Global and regional anthropogenic sulfur dioxide emissions. *Global and Planetary Change*, 29(1-2), 99–119.

Sokhi, R., Gray, C., Gardiner, K., & Earwaker, L. (1990). PIXE analysis of carbon black for elemental impurities. *Nuclear Instruments and Methods in Physics Research Section B: Beam Interactions with Materials and Atoms*, 49(1-4), 414–417.

Srivastava, R. K., Jozewicz, W., & Singer, C. (2001). SO2 scrubbing technologies: A review. *Environmental Progress*, 20(4), 219–228.

Suman, D. O., Kuhlbusch, T. A. J., & Lim, B. (1997). Marine sediments: A reservoir for black carbon and their use as spatial and temporal records of combustion. In *Sediment Records of Biomass Burning and Global Change* (pp. 271–293). Springer Science + Business Media.

Thevenon, F. & Anselmetti, F. S. (2007). Charcoal and fly-ash particles from lake lucerne sediments (central Switzerland) characterized by image analysis: anthropologic, stratigraphic and environmental implications. *Quaternary Science Reviews*, 26(19-21), 2631–2643.

Valette-Silver, N. J. (1993). The use of sediment cores to reconstruct historical trends in contamination of estuarine and coastal sediments. *Estuaries*, 16(3), 577.

Institutionen för naturgeografi och ekosystemvetenskap, Lunds Universitet.

Student examensarbete (Seminarieuppsatser). Uppsatserna finns tillgängliga på institutionens geobibliotek, Sölvegatan 12, 223 62 LUND. Serien startade 1985. Hela listan och själva uppsatserna är även tillgängliga på LUP student papers (https://lup.lub.lu.se/student-papers/search/) och via Geobiblioteket (www.geobib.lu.se)

The student thesis reports are available at the Geo-Library, Department of Physical Geography and Ecosystem Science, University of Lund, Sölvegatan 12, S-223 62 Lund, Sweden. Report series started 1985. The complete list and electronic versions are also electronic available at the LUP student papers (https://lup.lub.lu.se/student-papers/search/) and through the Geo-library (www.geobib.lu.se)

372 Andreas Dahlbom (2016) The impact of permafrost degradation on methane fluxes - a field study in Abisko

373 Hanna Modin (2016) Higher temperatures increase nutrient availability in the High Arctic, causing elevated competitive pressure and a decline in *Papaver radicatum*

374 Elsa Lindevall (2016) Assessment of the relationship between the Photochemical Reflectance Index and Light Use Efficiency: A study of its seasonal and diurnal variation in a sub-arctic birch forest, Abisko, Sweden

375 Henrik Hagelin and Matthieu Cluzel (2016) Applying FARSITE and Prometheus on the Västmanland Fire, Sweden (2014): Fire Growth Simulation as a Measure Against Forest Fire Spread – A Model Suitability Study –

376 Pontus Cederholm (2016) Californian Drought: The Processes and Factors Controlling the 2011-2016 Drought and Winter Precipitation in California

377 Johannes Loer (2016) Modelling nitrogen balance in two Southern Swedish spruce plantations

378 Hanna Angel (2016) Water and carbon footprints of mining and producing Cu, Mg and Zn: A comparative study of primary and secondary sources

379 Gusten Brodin (2016) Organic farming's role in adaptation to and mitigation of climate change - an overview of ecological resilience and a model case study

380 Veränika Trollblad (2016) Odling av *Cucumis Sativus* L. med aska från träd som näringstillägg i ett urinbaserat hydroponiskt system

381 Susanne De Bourg (2016) Tillväxteffekter för andra generationens granskog efter tidigare genomförd kalkning

382 Katarina Crafoord (2016) Placering av energiskog i Sverige - en GIS analys

383 Simon Nåfält (2016) Assessing avalanche risk by terrain analysis An experimental GIS-approach to The Avalanche Terrain Exposure Scale (ATES)

384 Vide Hellgren (2016) Asteroid Mining - A Review of Methods and Aspects

385 Tina Truedsson (2016) Hur påverkar snömängd och vindförhållande vattentrycksmätningar vintertid i en sjö på västra Grönland?

386 Chloe Näslund (2016) Prompt Pediatric Care Pediatric patients' estimated travel times to surgically-equipped hospitals in Sweden's Scania County

387 Yufei Wei (2016) Developing a web-based system to visualize vegetation trends by a nonlinear regression algorithm

388 Greta Wistrand (2016) Investigating the potential of object-based image analysis to identify tree avenues in high resolution aerial imagery and lidar data

389 Jessica Ahlgren (2016) Development of a Web Mapping Application for grazing resource information in Kordofan, Sudan, by downloading MODIS data automatically via Python

390 Hanna Axén (2016) Methane flux measurements with low-cost solid state sensors in Kobbefjord, West Greenland

391 Ludvig Forslund (2016) Development of methods for flood analysis and response in a Web-GIS for disaster management

392 Shuzhi Dong (2016) Comparisons between different multi-criteria decision analysis techniques for disease susceptibility mapping

393 Thirze Hermans (2016) Modelling grain surplus/deficit in Cameroon for 2030

394 Stefanos Georganos (2016) Exploring the spatial relationship between NDVI and rainfall in the semi-arid Sahel using geographically weighted regression

395 Julia Kelly (2016) Physiological responses to drought in healthy and stressed trees: a comparison of four species in Oregon, USA

396 Antonín Kusbach (2016) Analysis of Arctic peak-season carbon flux estimations based on four MODIS vegetation products

397 Luana Andreea Simion (2016) Conservation assessments of Văcărești urban wetland in Bucharest (Romania): Land cover and climate changes from 2000 to 2015

398 Elsa Nordén (2016) Comparison between three landscape analysis tools to aid conservation efforts

399 Tudor Buhalău (2016) Detecting clear-cut deforestation using Landsat data: A time series analysis of remote sensing data in Covasna County, Romania between 2005 and 2015

400 Sofia Sjögren (2016) Effective methods for prediction and visualization of contaminated soil volumes in 3D with GIS

401 Jayan Wijesingha (2016) Geometric quality assessment of multi-rotor unmanned aerial vehicle-borne remote sensing products for precision agriculture

402 Jenny Ahlstrand (2016) Effects of altered precipitation regimes on bryophyte carbon dynamics in a Peruvian tropical montane cloud forest

403 Peter Markus (2016) Design and development of a prototype mobile geographical information system for real-time collection and storage of traffic accident data

404 Christos Bountzouklis (2016) Monitoring of Santorini (Greece) volcano during post-unrest period (2014-2016) with interferometric time series of Sentinel-1A

405 Gea Hallen (2016) Porous asphalt as a method for reducing urban storm water runoff in Lund, Sweden

406 Marcus Rudolf (2016) Spatiotemporal reconstructions of black carbon, organic matter and heavy metals in coastal records of south-west Sweden